The role of Rnf in Ion gradient Formation in *Desulfovibrio alaskensis*

Luyao Wang, Peter Bradstock, Chuang Li, Michael J McInerney, Lee R Krumholz

Rnf is a membrane protein complex that has been shown to be important in energy conservation. Here, *Desulfovibrio alaskensis* G20 and Rnf mutants of G20 were grown with different electron donor and acceptor combinations to determine the importance of Rnf in energy conservation and the type of ion gradient generated. Addition of the protonophore TCS strongly inhibited lactate-sulfate dependent growth whereas the sodium ionophore ETH2120 had no effect, indicating a role for the proton gradient during growth. Mutants in *rnfA* and *rnfD* were more sensitive to the protonophore at 5 µM than the parental strain, suggesting the importance of Rnf in the generation of a proton gradient. The electrical potential (ΔΨ), ΔpH and proton motive force were lower in the *rnfA* mutant than in the parental strain of *D.alaskensis* G20. These results provide evidence that the Rnf complex in *D. alaskensis* functions as a primary proton pump whose activity is important for growth.

The role of Rnf in Ion gradient Formation in *Desulfovibrio alaskensis*

Luyao Wang[1], *Peter Bradstock*[1], *Chuang Li*[1], *Michael J. McInerney*[1], *Lee R. Krumholz*[1,2*],

Department of Microbiology and Plant Biology[1] and Institute for Energy and the Environment[2],

The University of Oklahoma, Norman, OK 73019 and

Running title:

*Corresponding author:

Department of Microbiology and Plant Biology, The University of Oklahoma,

770 Van Vleet Oval, Norman, OK 73019, USA

Tel: 405-325-0437 Fax: 405-325-7619 Email: krumholz@ou.edu

Contents category: Microbial metabolism

ABSTRACT

Rnf is a membrane protein complex that has been shown to be important in energy conservation. Here, *Desulfovibrio alaskensis* G20 and Rnf mutants of G20 were grown with different electron donor and acceptor combinations to determine the importance of Rnf in energy conservation and the type of ion gradient generated. Addition of the protonophore TCS strongly inhibited lactate-sulfate dependent growth whereas the sodium ionophore ETH2120 had no effect, indicating a role for the proton gradient during growth. Mutants in *rnfA* and *rnfD* were more sensitive to the protonophore at 5 μM than the parental strain, suggesting the importance of Rnf in the generation of a proton gradient. The electrical potential ($\Delta\Psi$), ΔpH and proton motive force were lower in the *rnfA* mutant than in the parental strain of *D.alaskensis* G20. These results provide evidence that the Rnf complex in *D. alaskensis* functions as a primary proton pump whose activity is important for growth.

The Rnf complex was first discovered in *Rhodobacter capsulatus* and is thought to be transcribed in one cluster of seven genes *rnf*ABCDGEH (Jouanneau et al., 1998). Evidence that depleting one subunit could destabilize others indicated the formation of a complex (Kumagai et al., 1997) which was later shown to be a protein complex involved in the *Rhodobacter* nitrogen fixation process (Schmehl et al., 1993). The Rnf complex has been differentiated into three major groups based on gene organization (Biegel et al., 2011). The first group found in *R. capsulatus*, *Pseudomonas stutzeri* (Yan et al., 2008) and *Azotobacter vinelandii* (Curatti et al., 2005) with *rnf*ABCDGE. Another group with the gene order *rnf*CDGEAB is found in *A.woodii* (Biegel et al., 2009) and *Clostridium kluyveri* (Seedorf et al., 2008). Lastly *rnf*BCDGEA is found in *Chlorobium limicola, Bacteroides vulgatus* and *Prosthecochloris aestuarii* (Biegel et al., 2011).

Rnf complex has been shown to be a novel type of ferredoxin-dependent enzyme, catalyzing the oxidation-reduction reaction between reduced ferredoxin and NAD^+ (Biegel et al., 2009; Boiangiu et al., 2005). Because of the high sequence similarity to the Na^+-translocating NADH:ubiquinone oxidoreductase (Nqr) (Kumagai et al., 1997), the Rnf complex in *R. capsulatus* was suggested to be involved in ion translocation using the energy from the exergonic reduction of NAD^+ coupled to the oxidation of reduced ferredoxin (Müller et al., 2008). Based on the above similarity, Rnf was originally proposed to be a sodium pump (Biegel et al., 2009). This theory was strengthened after the Rnf complex in *Acetobacterium woodii* was confirmed to generate a Na^+ gradient when carrying out the redox reaction between reduced ferredoxin and NAD^+ (Biegel & Müller, 2010). However, the Rnf complex was

suggested to be a proton-translocating ferredoxin:NAD^+ oxidoreductase in *Clostridium ljungdahlii* (Kopke et al., 2010) and was more recently shown to produce a proton gradient (Tremblay et al., 2013). It therefore appears that Rnf may pump different ions in different bacteria (Hess et al., 2016).

Desulfovibrio alaskensis G20 encodes the Rnf complex with a unique gene arrangement (*rnf*CDGEABF); however, a similar Rnf complex is present in most sulfate-reducing bacteria for which genome sequences are available (Pereira et al., 2011). Directly preceding the operon is a decaheme cyctochrome (dhcA) which is also present in many but not all sulfate reducing bacteria The first gene in the *rnf* operon is a decaheme cytochrome (DhcA) that belongs to cytochrome c_3 family (Pereira et al., 2011). The final gene in the operon, *rnf*F is most similar to *apb*E, a membrane associated lipoprotein (Beck & Downs, 1999).

Recently, it was reported that mutants in Rnf in *D. alaskensis* are unable to grow using H_2 or during syntrophic growth conditions with *Syntrophus aciditrophicus* or *Syntrophomonas wolfeii* (Krumholz et al., 2015; Price et al., 2014). By investigating gene expression levels of *D.alaskensis* G20 grown in pure culture or under syntrophic conditions (Krumholz et al., 2015), it was suggested that both formate and H_2 can act as electron shuttles during syntrophic growth. Those experiments also showed that expression of *rnf* genes are upregulated under syntrophic conditions and during H_2 dependent growth confirming the role of the Rnf complex in H_2 metabolism.

In this experiment, mutants of RnfA (Dde_0585) and RnfD (Dde_0582) were studied and compared with the G20 parent strain to determine whether Rnf in *D. alaskensis* is involved in generation of a proton motive force (PMF). These two

mutants of *Desulfovibro alaskensis* G20 were obtained by using mini Tn10 transposon (Groh et al., 2005) and identified individually during syntrophic growth with *Syntrophomonas wolfeii* (Krumholz et al., 2015).

MATERIALS AND METHODS

Growth of Cultures. *Desulfovibrio alaskensis* G20 and *rnf* mutants were routinely cultured anaerobically (N_2-CO_2, 80:20) in basal medium with lactate-sulfate (50mM each) as the electron donor and electron acceptor, respectively and contained 0.1% yeast extract (Krumholz et al., 2015). The medium was prepared under a headspace of N_2/CO_2 (80/20, vol/vol) with sodium bicarbonate (3.5g/L) added as a buffer. Before inoculation, the medium was reduced with 0.025% each cysteine and sulfide. Kanamycin (1050 μg/mL) was added to the mutant cultures. Inoculum consisted of 0.2 ml transferred into 10 ml of media or the same ratio for large volume cultures. Cultures were grown in the incubator at 37°C and growth of triplicate cultures was measured by optical density at 600 nm. The stock cultures were frozen in 20% glycerol at -20°C. Growth of syntrophic cocultures was as previously described (Krumholz et al., 2015).

Growth was tested with a variety of other electron donors and acceptors: lactate (50mM), pyruvate (25mM), ethanol (10mM) and formate (50mM). Sulfate was used at 50mM with lactate and 25mM with other electron donors and sulfite was added at 10mM.

The protonophore 3,3,4,5-tetrachlorosalicylanide (TCS, 5 μM or 20 μM), or the sodium-specific ionophore N,N,N′,N′-Tetracyclohexyl-1,2-phenylenedioxydiacetamide (ETH2120, 20 μM) were added to media to test their effects on growth.

111

112 **Transcriptional analysis of *rnf* genes.** Total RNA was extracted from the parent strain,
113 *rnfA*, and *rnfD* mutants using the Qiagen RNeasy kit as previously described (Krumholz
114 et al., 2015). Purity and adequate yield was confirmed with a diode-array
115 spectrophotometer. First-strand cDNA synthesis was performed using the Fermentas
116 Revertaid kit with gene-specific primers covering the entirety of the *rnf* mutants'
117 operons . Primers were designed to span the gaps between each gene in the operon
118 (Table 1). PCR was performed with the parent strain and mutants with each primer set
119 followed by agarose gel analysis to determine whether all genes in the operon were
120 expressed and whether the genes were on the same transcript.
121 *Quantitative PCR analysis.* Triplicate cultures of the parent strain and *rnfA* and *rnfD*
122 mutants were grown to mid-log phase (OD_{600} 0.3-0.45) and harvested by centrifugation
123 at 5,000 x g for 5 min at 4 °C. The pellet was homogenized in RNAprotect Bacteria
124 reagent (QIAGEN) for 5 min at room temperature to prevent degradation of RNA
125 transcripts. Excess liquid was removed by centrifugation and cell pellets were
126 resuspended in 200ul of TE buffer containing 1mg/ml lysozyme. Total RNA was
127 extracted using the RNeasy mini kit (QIAGEN). RNA was then treated with the
128 Ambion Turbo DNA –free kit (Thermo) to eliminate genomic DNA contamination.
129 RNA was quantified spectrophotometrically. cDNAs were synthesized using the First
130 Stand cDNA synthesis kit (Fermentas) as described in the manual. Control PCR
131 reactions were done to ensure there was no genomic DNA or non-specific
132 amplification.

Quantitative PCR, was done in triplicate from each culture replicate using 10ng cDNA as the template and the Maxima SYBR Green qPCR master mix (Thermo) with a MyIQ Cycler (Bio-Rad). Primers were designed using Primer-BLAST (NCBI website) to specifically amplify 128- to 155-bp regions of targeted genes Dde_587, Dde_589, Dde_590 (Table 2). Dde_0587 is the final gene in the *rnf* operon and the other two genes are the next two ORFs directly downstream of the operon. The 16s rRNA primers were as previously described (Li et al., 2011). Reactions used the following amplification condition: 95°C for 10 min; 40 cycles of denaturation at 95°C for 15 s and annealing/extension at 60°C for 1 min. mRNA expression was calculated using $(E_{target})^{\Delta Ct_target\ (control-\ mutant)} / (E_{reference})^{\Delta Ct_reference\ (control-\ mutant)}$ (Pfaffl, 2001) The 16s rRNA gene was used for normalization.

Washed cell experiments. Washed cells were used to measure sulfide production under non-growth conditions. Briefly, 100 ml lactate-sulfate culture grown to mid log phase was harvested by centrifugation at 5300 x g for 15 min, washed twice in buffer containing 50 mM MOPS (pH 7.2), 5 mM $MgCl_2$ and resuspended in the same buffer. All buffers were flushed with N_2 for 30 min. Assays were carried out in serum tubes containing 2 ml of buffer-cell mixture incubated at 37^{o}C on a shaker at 100rpm. The assay mixture contained the washing buffer, 5mM sodium sulfate and either 50 mM lactate, 50 mM sodium formate (N_2 headspace) or H_2 in the headspace. Between 50 and 200 μg of cell protein was added to each tube. Tubes were sacrificed by addition of 2 ml 10% Zinc Acetate at 60 min intervals for sulfide analysis. Sulfide was determined using the methylene blue assay (Cline, 1969).

Measurement of proton motive force. Triplicate cultures of *D. alaskensis* parent strain and *rnf*A mutant were grown in lactate –sulfate basal medium until mid exponential phase (OD_{600} of 0.5) in a 1 liter volume and 30 ml aliquots of cells were dispensed into 100ml serum bottles under N_2/CO_2 (80/20, vol/vol). The basal medium contains 5 mM K^+, mainly added as potassium phosphate salts. Protein concentration was determined using the Bicinchoninic Acid Assay (Pierce BCA Protein Assay Kit).

Transmembrane electrical potential ($\Delta\Psi$) was measured as previously described (Tremblay et al., 2013). Briefly, cells were incubated with [^{3}H]tetraphenylphosphonium bromide ([^{3}H]TPP^+) (ARC, 0.1µCi/ml) for 15 min at 37°C (Kashket & Barker, 1977; Shirvan et al., 1989). [^{3}H]TPP^+ was dissolved in media and filtered through 0.45 µm filters prior to adding to cells. Controls were incubated with nigericin (ACROS ORGANICS, 20µM dissolved in ethanol at 200x) and valinomycin (ACROS), 20µM dissolved in DMSO at 200x) for 15 min to eliminate the $\Delta\Psi$. The combination of nigericin (proton/K^+ antiporter) and valinomycin (K^+ uncoupler) will dissipate the proton gradient (Kessler et al., 1977). Cells were then separated from the medium using silicone oil as described below and [^{3}H]TPP^+ was determined in the liquid scintillation counter (Packard TriCarb 2100TR). The uptake of [^{3}H]TPP^+ was corrected for extracellular contamination using the ratio of the intracellular to extracellular volume as described below. Non-specific binding of [^{3}H]TPP^+ was corrected by subtracting the cell associated [^{3}H]TPP^+ in the valinomycin/nigericin treatment from that in the untreated cells. The $\Delta\Psi$ was calculated with the simplified Nernst equation (-2.3 [RT/F]×log[(concentration in)/(concentration out)]).

177 The ΔpH was measured by testing the distribution of [^{14}C]benzoate (ARC,
178 0.4μCi/ml) across the cell membrane after 15min incubation at 37°C with cells
179 (Kashket & Barker, 1977; Shirvan et al., 1989). Cells were then separated from the
180 supernatant as described below and [^{14}C]benzoate was measured. [^{14}C]benzoate
181 uptake was corrected for extracellular contamination using the ratio of intracellular to
182 extracellular volume described below. Tetrachlorosalicylanilide (TCS, 20μM) was
183 added to controls to eliminate the ΔpH and was used to calculate internal pH in the
184 absence of a ΔpH. The external pH was measured, [^{14}C]benzoate uptake was
185 quantified and intracellular pH was calculated with the Henderson–Hasselbach equation
186 (Rottenberg, 1979). The proton motive force (PMF) was calculated using the
187 equation: PMF=ΔΨ-zΔpH. At 37°C, z equals to 61.48.

188 ***Measurement of intracellular volume/total volume of cell pellet.*** $^{3}H_2O$ （1μCi/ml)
189 was used to measure the total pellet volume while [^{14}C]taurine (PerkinElmer, 0.5μCi/ml)
190 was used to measure extracellular volume and was inferred to penetrate up to the
191 plasma membrane (Kashket & Barker, 1977). The intracellular water volume was
192 estimated from total pellet water volume minus extracellular water volume by
193 measuring the difference between the distribution of $^{3}H_2O$ and [^{3}H]taurine after
194 incubating cells for 15 min at 37°C with each isotope.

195 ***Separation of cells from the supernatant.*** Following the 15 minute incubation with
196 the isotope, three 10 ml aliquots of the total 30 ml solution were put into three 15 ml
197 Falcon tubes with 3ml of a mixture of silicone oils (25% Fluid 510, 50 centistokes, and
198 75% Fluid 550, 115 centistokes; Dow-Corning Corp, Serva. vol/vol). Cells were then
199 centrifuged at 5300 x g at 4°C for 10min. The aqueous layer and the silicone oil was

removed with a Pasteur pipette connected to a vacuum line. The bottom of the falcon tube containing the cell pellet was cut off and moved into the scintillation vial and the cell pellet was re-suspended with 200µl distilled-water. Liquid scintillation cocktail (PerkinElmer, Ultima Gold) was added prior to scintillation counting.

Statistical analysis. Statistical analysis used either the t-test or a one-way analysis of variance (ANOVA) with the Tukey's Range test.

RESULTS

Mutants in the rnf operon. In a previous study, a Tn10 mutant library of *D. alaskensis* G20 was screened for the ability to grow on butyrate in coculture with *Syntrophomonas wolfei* (Krumholz et al., 2015). Seventeen mutants were obtained that were deficient in syntrophic growth. Of these, two mutants had the transposon insertions within a putative *rnf* operon. This operon is composed of 8 genes located on the genome as shown in Table 3 and genes appear to be co-transcribed. They are separated from the nearest upstream transcribed region by 185 bps and from the nearest downstream transcribed region by 342 bps. The two syntrophy mutants had transposon insertions within *rnf*A and *rnf*D as determined using Arbitrary PCR (Krumholz et al., 2015). Both genes encode integral membrane proteins likely located in the cytoplasmic membrane. RnfD has been previously shown to bind a flavin (Biegel et al., 2011).

Transcriptional analysis of the rnf operon. The complete transcriptional analysis for strain G20 under lactate-sulfate, H_2-sulfate and under syntrophic growth conditions has been previously published (Krumholz et al., 2015). Here we present a summary of normalized values for transcription of each subunit within the *rnf* operon (Table 3).

Transcription of all genes in the operon including *dchA* are similar under each condition and are affected similarly by growth condition. The most highly expressed genes are the first two in the operon, the gene for the cytochrome c family protein and *rnf*C, both of which have 1.5-2 fold higher levels of expression than genes for the other subunits. Expression was also enhanced approximately 2-fold when cultures were grown on H_2, relative to lactate, indicating the importance of this protein for H_2 dependent growth. Syntrophic cultures had enhanced expression of all eight genes compared to lactate/sulfate growth with similar levels of expression in the *S. aciditrophicus* coculture to H_2-grown cells and higher levels of expression observed in the *S. wolfei* coculture, indicating the importance of this protein complex under syntrophic conditions. Similar effects on transcription provide evidence that all eight genes are located in one operon.

Expression analysis of rnf operons in mutants. To determine whether the transposon insertion eliminated downstream expression of genes in the *rnf* operon, gap analysis was performed where all intergene regions were amplified except the region between *rnfB* and *rnfA* using cDNA prepared using mRNA. All of the intergene regions were amplified for the parent and the two mutants (Fig. S1) confirming that all 8 genes form an operon and indicating that the mutants likely have intact transcripts of the interrupted operon. In this operon, the insertions are likely only affecting the one interrupted gene.

We carried out RT-PCR analysis of the terminal gene in the operon, Dde_587 (*rnfF*) as well as the two genes that followed that operon, Dde_589 (*uspA*) and Dde_590 (*cls*) to be certain that downstream expression was not affected by the insertions. Expression of the terminal gene in the operon was impacted in the mutants with a

246 4 fold decrease in expression in the *rnfA* mutant and a 2 fold increase in the *rnfD*
247 mutant (Table 4). The following 2 genes were minimally impacted indicating that
248 the insertions present in the mutants likely do not affect downstream expression.
249 ***Growth and sulfate reduction by rnf mutants.*** The two mutants exhibited similar
250 growth rates to that of the parent strain when lactate was the electron donor with sulfate
251 (Fig. 1A) or sulfite as electron acceptor (Fig. 1B). When pyruvate was the donor,
252 growth yields were reduced for the mutants (Fig. 1C). We previously reported that *rnf*
253 mutants grew poorly (*rnf*D) or not at all (*rnf*A) on H_2 (Krumholz et al., 2015) and a
254 recent study has reported that rnf mutants grow poorly or not at all with sulfate as the
255 electron acceptor on malate, fumarate, ethanol, hydrogen, and formate, but growth is
256 not affected in lactate and pyruvate (Price et al., 2014). Here, it is shown that the *rnfD*
257 mutant has a long lag phase with formate as the donor, but eventually grew to a similar
258 OD to the parent strain (Fig. 1D). The *rnfA* mutant did not grow on formate or H_2
259 clearly indicating the involvement of Rnf in formate/H_2-dependent growth. We also
260 confirmed that the *rnfA* mutant will not grow on ethanol (Fig. S3).
261 ***Sulfide production by washed cells.*** Washed cells were used to determine if the role for
262 *rnf* was linked to biosynthesis, as mutants were able to grow better on more complex
263 carbon compounds. Incubations of washed cells of the parent strain and the *rnfA*
264 mutant produced 0.57 and 0.17 μmol sulfide.hr^{-1}.mg^{-1} protein respectively with lactate
265 as electron donor. Addition of either 5 μM TCS to the washed cells of the parent
266 strain prevented 95% of the sulfide production and addition of 20μM to washed cells
267 inhibited sulfide production by 100%, suggesting TCS directly disrupts the proton
268 gradient needed for respiration. With H_2 as the electron donor, parent strain cells

produced 0.30 μmol sulfide.hr^{-1}.mg^{-1} protein whereas the *rnfA* mutant did not have any detectable activity. To further test whether the lack of growth on H_2 was due to the mutant's inability to biosynthesize carbon intermediates, we attempted to grow the mutant and the parent strain with H_2 as the electron donor with 0.1% Casamino acids added to the media. The mutant would still not grow (Fig. S4), providing further evidence that the role for RNF was not directly linked to biosynthesis.

Growth curves with ionophores. The sodium ion ionophore ETH 2120, tested at 20 μM, did not have a significant influence on the growth of the parent strain or the *rnf* mutants with lactate as the electron donor whether sulfate or sulfite were present as electron acceptors (Fig S5,S6). Interestingly, the protonophore, TCS , at 5 μM differentially inhibited cultures (Fig. 2). TCS partially inhibited the growth of the parent strain and completely inhibited the growth of *rnf* mutants on lactate-sulfate (Fig. 2A and Fig. S5). Growth on lactate sulfite was then tested and 5 μM TCS was shown to have a smaller but still significant inhibitory effect on growth in the parent strain (Fig. 2B) and again completely inhibited the *rnfA* mutant (Fig. 2B, S6). A higher level of TCS was then tested and it was shown that 20 μM TCS almost completely inhibited the growth of the parent strain on lactate-sulfite (Fig. 2B) and again completely inhibited the mutants (Fig. S7).

Measurement of ΔΨ, ΔpH and PMF. To determine whether the Rnf complex is involved in the formation of a proton gradient, the transmembrane potential (ΔΨ), ΔpH and proton motive force (PMF) were measured in cells of the G20 parent strain and the *rnf*A mutant growing on lactate-sulfate. The ΔΨ and ΔpH were both reduced in the mutant (Table 5), which led to a significantly lower PMF in the *rnfA* mutant relative to

292 the G20 parent strain. The lower ΔpH and PMF in the *rnfA* mutant shows that the Rnf
293 complex clearly had an impact on the energy conservation system by affecting the
294 proton gradient.

295 **DISCUSSION**

296 The Rnf complex has previously been shown to catalyze the oxidation-reduction
297 reaction between ferredoxin and NAD^+ (Biegel et al., 2009; Boiangiu et al., 2005). The
298 redox potential of bacterial ferredoxin can vary, but has been reported within the range
299 of -385 to -460 mV (Smith & Feinberg, 1990). That is more negative than that of
300 NAD^+/NADH couple (E'=-280mV) and therefore the transfer of electrons by Rnf from
301 reduced ferredoxin to NAD^+ releases sufficient energy to generate either a proton or a
302 sodium ion potential (Buckel & Thauer, 2013). Given that recent studies have
303 demonstrated both proton (Tremblay et al., 2013) and Na^+ translocation abilities (Biegel
304 & Müller, 2010), it was imperative to determine which ion Rnf translocates in strain
305 G20. Growth experiments showed that lactate-sulfate grown cells were insensitive to
306 the Na^+ ionophore, ETH2120, (Figs. S5, S6) but were highly sensitive to the
307 protonophore, TCS (Fig. 2). Resting cells were also shown to be highly sensitive to
308 TCS suggesting that the proton gradient is needed for sulfate reduction. A similar
309 growth profile was observed in *C. ljungdahlii*, for which this result was interpreted to
310 infer that a proton gradient was needed for growth (Tremblay et al., 2013). . ..

311 When grown on lactate-sulfate or lactate-sulfite, TCS partially inhibited the growth
312 of the parent strain and completely inhibited the growth of *rnfA and rnfD* mutants (Fig.
313 2). The stronger effect on the mutants suggested that TCS at 5 μM was partially
314 dissolving the proton gradient in the parent strain and this was confirmed when cells

were shown to be completely inhibited at 20μM TCS. We would therefore expect that at 5 μM TCS, growth processes requiring additional proton motive force (or ATP synthesis) would be more highly inhibited than those requiring less ATP. The use of sulfate as an electron acceptor initially requires energy to activate sulfate to adenosine-5'-phosphosulfate (Gavel et al., 1998). The requirement for energy to activate sulfate may explain why lactate-sulfate grown cells are more susceptible to the action of TCS than are lactate-sulfite-grown cells as the proton gradient generated during sulfate respiration would be needed to make ATP for sulfate activation. The inability of *rnf* mutants to grow in the presence of 5 uM TCS is consistent with its role in the generation of a proton motive force. In fact, the magnitude of the proton motive force in *rnf* mutants is much less than that in the parent strain of G20 (Table 5).

Ideally, we would have generated complemented *rnf* mutants to prove that the observed insertions were not having polar effects on other genes. We have attempted to clone the *rnfA* and *rnfD* genes into *Escherichia coli* as the first step in complementing the mutants. Unfortunately we have not been successful. Another group has experienced similar problems with *rnf*AB of *Clostridum ljungdahlii* and suggested that *rnf* genes may be toxic to *E. coli* in some cases *(Tremblay et al., 2013)*. Gap analysis was used to show that the insertions did not block transcription of downstream genes providing some evidence that polar effects are not important. As well, we carried out RT-PCR analysis of downstream genes. There was a decreased level of expression of the terminal gene in the Rnf operon (*rnfF*) by the *rnfA* mutant, however, there was little effect of the insertions (mutations) on expression of genes downstream of the operon.

338 Experiments reported here and elsewhere (Price et al., 2014) show that the *rnf*
339 mutants are unable to grow on H_2, formate and ethanol. These results point to a critical
340 role for Rnf during growth on the above substrates and are consistent with a higher
341 expression level of *rnf* genes when growing with H_2 and sulfate relative to lactate and
342 sulfate (Table 3).

343 A proton gradient is thought to be generated during H_2 metabolism in *Desulfovibrio*
344 (Badziong & Thauer, 1980) and used for the synthesis of ATP. Membrane vesicle
345 experiments carried out in our lab in an attempt to demonstrate the generation of an ion
346 gradient coupled to the oxidation of reduced ferredoxin and reduction of NAD^+ have
347 been unsuccessful. The protein product of the decaheme cytochrome that precedes the
348 *rnf* operon has been proposed to accept electrons from hydrogenases and shuttle them to
349 Rnf (Matias et al., 2005; Pereira et al., 2011). However, mutants in this gene had no
350 effect on fitness during growth experiments on ethanol, formate or H_2 (Price et al.,
351 2014). This suggests that Rnf is not likely receiving electrons directly from H_2. It is
352 more likely that *D. alaskensis* relies extensively on ferredoxin oxidation by Rnf to
353 produce a proton gradient during growth on substrates that do not yield net ATP by
354 substrate-level phosphorylation. For those substrates that do yield ATP by substrate
355 level phosphorylation such as malate, fumarate, pyruvate and lactate, a decreased
356 growth rate and or yield was observed in most cases for rnf mutants (Fig. 1)(Price et al.,
357 2014) suggesting that both Rnf and the F1Fo ATPase are involved in generating a PMF
358 under those conditions.

359 We are not familiar with any studies describing mechanisms of ferredoxin
360 reduction in *Desulfovibrio,* however, several possible mechanisms have been suggested

(Pereira et al., 2011; Price et al., 2014). During H_2 oxidation, these include a possible cytoplasmic electron-bifurcating hydrogenases-linked to a heterodisulfide reductase for which mutants grow poorly on H_2 and formate (Hdr/flox-1). For ethanol oxidation, the acetaldehyde:ferredoxin oxidoreductase could be used, and with pyruvate and lactate oxidation, would involve pyruvate:ferredoxin oxidoreductase.

Results from this study are consistent with the fact that *D. alaskensis* Rnf complex functions as a proton rather than a sodium pump and is essential for growth on substrates that do not involve ATP synthesis by substrate-level phosphorylation. Mutation of Rnf limits the development of the PMF and, thus, affects ATP synthesis during growth.

REFERENCES

Badziong W, and Thauer RK. 1980. Vectorial electron transport in *Desulfovibrio vulgaris* (Marburg) growing on hydrogen plus sulfate as sole energy source. Archives of Microbiology 125:167-174.

Beck BJ, and Downs DM. 1999. A periplasmic location is essential for the role of the ApbE lipoprotein in thiamine synthesis in *Salmonella typhimurium*. Journal of Bacteriology 181:7285-7290.

Biegel E, and Müller V. 2010. Bacterial Na^+-translocating ferredoxin: NAD^+ oxidoreductase. Proceedings of the National Academy of Sciences 107:18138-18142.

Biegel E, Schmidt S, González JM, and Müller V. 2011. Biochemistry, evolution and physiological function of the Rnf complex, a novel ion-motive electron transport complex in prokaryotes. Cellular and Molecular Life Sciences 68:613-634.

Biegel E, Schmidt S, and Müller V. 2009. Genetic, immunological and biochemical evidence for a Rnf complex in the acetogen *Acetobacterium woodii*. Environmental Microbiology 11:1438-1443.

Boiangiu CD, Jayamani E, Brügel D, Herrmann G, Kim J, Forzi L, Hedderich R, Vgenopoulou I, Pierik A, and Steuber J. 2005. Sodium ion pumps and hydrogen production in glutamate fermenting anaerobic bacteria. Molecular Microbiology and Biotechnology 10:105-119.

Buckel W, and Thauer RK. 2013. Energy conservation via electron bifurcating ferredoxin reduction and proton/Na^+ translocating ferredoxin oxidation. Biochimica et Biophysica Acta (BBA)-Bioenergetics 1827:94-113.

Cline JD. 1969. Spectrophotometric determination of hydrogen sulfide in natural waters. Limnology and Oceanography 14:454-458.

Curatti L, Brown CS, Ludden PW, and Rubio LM. 2005. Genes required for rapid expression of nitrogenase activity in *Azotobacter vinelandii*. Proceedings of the National Academy of Sciences 102:6291-6296.

Gavel OY, Bursakov SA, Calvete JJ, George GN, Moura JJG, and Moura I. 1998. ATP sulfurylases from sulfate-reducing bacteria of the genus *Desulfovibrio*. A novel metalloprotein containing cobalt and zinc. Biochemistry 37:16225-16232.

Groh JL, Luo Q, Ballard JD, and Krumholz LR. 2005. A method adapting microarray technology for signature-tagged mutagenesis of *Desulfovibrio desulfuricans* G20 and *Shewanella oneidensis* MR-1 in anaerobic sediment survival experiments. Applied and Environmental Microbiology 71:7064-7074.

Hess V, Gallegos R, Jones JA, Barquera B, Malamy MH, and Muller V. 2016. Occurrence of ferredoxin: $NAD^{(+)}$ oxidoreductase activity and its ion specificity in several Gram- positive and Gram- negative bacteria. Peerj 4:e1515; DOI 10.7717/peerj.1515.

Jouanneau Y, Jeong HS, Hugo N, Meyer C, and Willison JC. 1998. Overexpression in *Escherichia coli* of the rnf genes from *Rhodobacter capsulatus*--characterization of two membrane-bound iron-sulfur proteins. European Journal of Biochemistry 251:54-64.

Kashket E, and Barker SL. 1977. Effects of potassium ions on the electrical and pH gradients across the membrane of *Streptococcus lactis* cells. Journal of Bacteriology 130:1017-1023.

Kessler RJ, Vande Zande H, Tyson CA, Blondin GA, Fairfield J, Glasser P, and Green DE. 1977. Uncouplers and the molecular mechanism of uncoupling in mitochondria. Proc Natl Acad Sci U S A 74:2241-2245.

Kopke M, Held C, Hujer S, Liesegang H, Wiezer A, Wollherr A, Ehrenreich A, Liebl W, Gottschalk G, and Durre P. 2010. *Clostridium ljungdahlii* represents a microbial production platform based on syngas. Proc Natl Acad Sci U S A 107:13087-13092.

Krumholz LR, Bradstock P, Sheik CS, Diao Y, Gazioglu O, Gorby Y, and McInerney MJ. 2015. Syntrophic growth of *Desulfovibrio alaskensis* requires genes for H_2 and formate metabolism as well as those for flagellum and biofilm formation. Applied and Environmental Microbiology 81:2339-2348.

Kumagai H, Fujiwara T, Matsubara H, and Saeki K. 1997. Membrane localization, topology, and mutual stabilization of the rnfABC gene products in *Rhodobacter capsulatus* and implications for a new family of energy-coupling NADH oxidoreductases. Biochemistry 36:5509-5521.

Li X, McInerney MJ, Stahl DA, and Krumholz LR. 2011. Metabolism of H_2 by *Desulfovibrio alaskensis* G20 during syntrophic growth on lactate. Microbiology 157:2912-2921.

Matias PM, Pereira IAC, Soares CM, and Carrondo MA. 2005. Sulphate respiration from hydrogen in *Desulfovibrio* bacteria: a structural biology overview. Progress in Biophysics and Molecular Biology 89:292-329.

Müller V, Imkamp F, Biegel E, Schmidt S, and Dilling S. 2008. Discovery of a ferredoxin:NAD^+-oxidoreductase (Rnf) in *Acetobacterium woodii*: a novel potential coupling site in acetogens. Annals of the New York Academy of Sciences 1125:137-146.

Pereira IAC, Ramos AR, Grein F, Marques MC, Da Silva SM, and Venceslau SS. 2011. A comparative genomic analysis of energy metabolism in sulfate reducing bacteria and archaea. Frontiers in Microbiology 2:1-22.

Pfaffl MW. 2001. A new mathematical model for relative quantification in real-time RT-PCR. Nucleic Acids Res 29:e45.

Price MN, Ray J, Wetmore KM, Kuehl JV, Bauer S, Deutschbauer AM, and Arkin AP. 2014. The genetic basis of energy conservation in the sulfate-reducing bacterium *Desulfovibrio alaskensis* G20. Frontiers in Microbiology 5:577. doi: 510.3389/fmicb.2014.00577.

Rottenberg H. 1979. The measurement of membrane potential and Δ pH in cells, organelles, and vesicles. Methods in enzymology 55:547-569.

Schmehl M, Jahn A, Meyer zu Vilsendorf A, Hennecke S, Masepohl B, Schuppler M, Marxer M, Oelze J, and Klipp W. 1993. Identification of a new class of nitrogen fixation genes in Rhodobacter capsalatus: a putative membrane complex involved in electron transport to nitrogenase. Molecular and General Genetics 241:602-615.

Seedorf H, Fricke WF, Veith B, Brüggemann H, Liesegang H, Strittmatter A, Miethke M, Buckel W, Hinderberger J, and Li F. 2008. The genome of *Clostridium kluyveri*, a strict anaerobe with unique metabolic features. Proceedings of the National Academy of Sciences 105:2128-2133.

Shirvan M, Schuldiner S, and Rottem S. 1989. Volume regulation in *Mycoplasma gallisepticum*: evidence that Na^+ is extruded via a primary Na^+ pump. Journal of Bacteriology 171:4417-4424.

Smith ET, and Feinberg BA. 1990. Redox properties of several bacterial ferredoxins using square wave voltammetry. J Biol Chem 265:14371-14376.

Tremblay P-L, Zhang T, Dar SA, Leang C, and Lovley DR. 2013. The Rnf complex of *Clostridium ljungdahlii* is a proton-translocating ferredoxin: NAD+ oxidoreductase essential for autotrophic growth. Mbio 4:e00406-00412.

Yan Y, Yang J, Dou Y, Chen M, Ping S, Peng J, Lu W, Zhang W, Yao Z, and Li H. 2008. Nitrogen fixation island and rhizosphere competence traits in the genome of root-associated *Pseudomonas stutzeri* A1501. Proceedings of the National Academy of Sciences 105:7564-7569.

Table 1. List of primers used for gap analysis in the *rnf* operon.

Gap	**Forward primer**	**Reverse primer**
Gap CC (*cytC/rnfC*)	GGCATTCACGGCCTGTGCCT	CTTGTCGCCGGGGTGATCGG
Gap CD (*rnfC/rnfD*)	CCTGCTGGGACGCTACAGCG	ATGCCGTGTATGGTGCGCCC
Gap DG (*rnfD/rnfG*)	GGCAAGGCCGCCATGGTCAT	TGTACTCGGCCCCCGTGGAG
Gap GE (*rnfG/rnfE*)	ATCGGCTGCATGGTTGCCGT	ATTGGCGGACTTGGTGACCG
Gap EA (*rnfE/rnfA*)	GGGCTTGTTCTGGGCGCCAT	CCGCCCATGCCCAGACTGAC
Gap BE (*rnfB/rnfF*)	AAAGCCTGCCTCGCGTTCGG	AAGCCCCAGCAGACCGCATG

Table 2. Primers used for the RT-qPCR experiments

Primer	Sequence	Target gene
Dde_587 forward	5'-AACCGTGGGTTATCGCCATT-3'	*rnfF* gene
Dde_587 reverse	5'-ATGGCTGTACATGCGTTTGC-3'	
Dde_589 forward	5'-AAGGGCAGGTAGTGCTGATG-3'	Putative regulator gene
Dde_589 reverse	5'-GGTAAACTTCACGCCTTCGC-3'	
Dde_590 forward	5'-GCCTGCGGCTTAATTTCGAG-3'	Cardiolipin synthase gene
Dde_590 reverse	5'-ACGGTTTTCCAGTTCGCTCA-3'	
16s forward	5'-ACGGTTGGAAACGACTGCTA-3'	16s rRNA gene
16s reverse	5'-AGCTAATCAGACGCGGACTC-3'	

Table 3. Normalized expression levels of genes within the *rnf* operon (from (Krumholz et al., 2015)). Expression was determined with the parent strain of *D. alaskensis* G20 during growth in pure culture with the indicated electron donors and acceptors and in coculture with *S. aciditrophicus* (SB) or with *S. wolfei* (SW) in the presence of benzoate or butyrate, respectively, as electron donors and sulfate as the electron acceptor.

Gene	Function	Lactate/ Sulfate	H_2/ Sulfate	H_2/ Sulfite	SB	SW
Dde_0580	cyt c family protein	3.17	8.33	6.18	6.02	14.36
Dde_0581	RnfC subunit	3.05	6.68	6.12	5.61	13.50
Dde_0582	RnfD subunit	1.90	4.41	3.34	2.68	7.73
Dde_0583	RnfG subunit	2.83	6.35	5.19	5.43	10.07
Dde_0584	RnfE subunit	1.86	4.95	3.80	3.39	7.63
Dde_0585	RnfA subunit	2.24	5.78	4.23	2.98	8.41
Dde_0586	RnfB subunit	2.18	4.39	4.16	1.48	8.09
Dde_0587	RnfF subunit	2.20	4.90	5.25	1.94	10.15

Table 4. Gene expression in *D. alaskensis rnfA* and *rnf D* mutants relative to the parental strain using RT-qPCR. And normalized with the 16s rRNA gene.

Mutant type	Dde_587	Dde_589	Dde_590
rnf A	0.227±0.255	0.608±0.097	0.589±0.253
rnf D	1.955±0.624	1.155±0.078	0.972±0.420

Table 5. Magnitude of the ΔpH, ΔΨ and total proton motive force of the D. alaskensis G20 parent strain and the *rnfA* mutant growing on lactate and sulfate. Standard deviation in parentheses. Value for the *rnfA* mutant were statistically different from the parent strain at $p<0.05$.

Measurement	Parent Strain	*rnf*A mutant
ΔΨ	-158 mV (2.1)	-117 mV (3.2)
ΔpH	0.43 (0.057)	0.29 (0.015)
PMF	-185 mV (3.1)	-135 mV (4.1)

532
533
534 **Figures**

Fig. 1

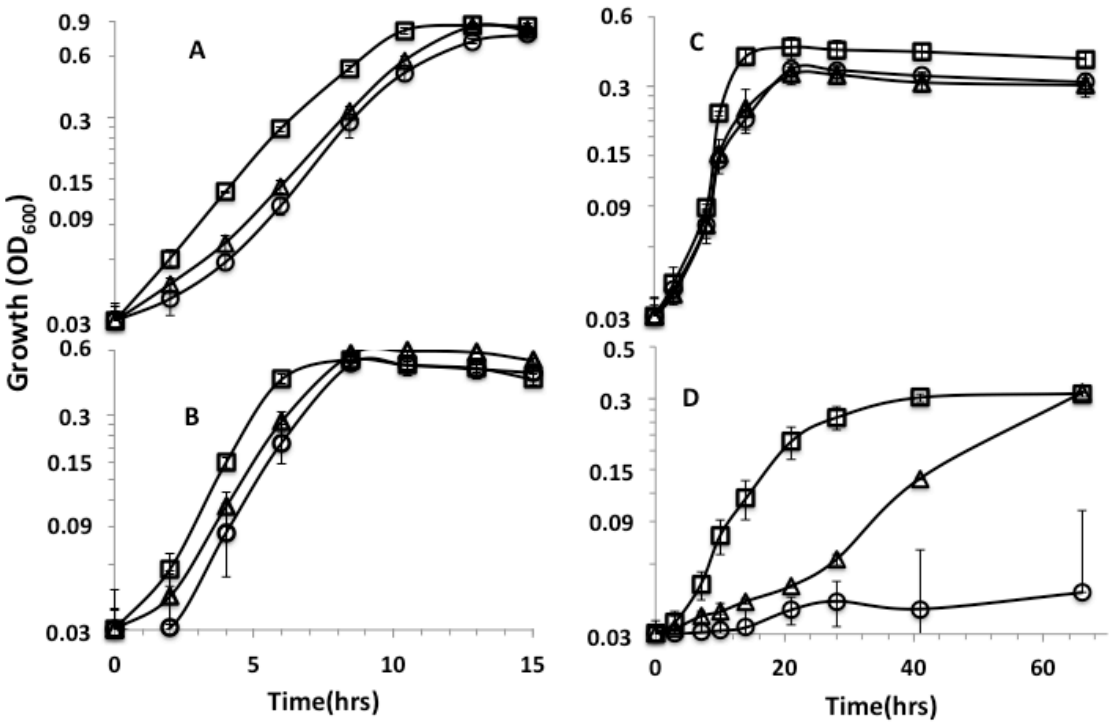

535
536 Figure 1. Growth curves on (A) lactate-sulfate (B) lactate-sulfite (C) pyruvate-sulfate
537 and (D) formate-sulfate. Curves are for *D. alaskensis* parent strain (□) *rnf*A (○) and
538 *rnf*D (△) mutants. Error bars show standard deviation.
539

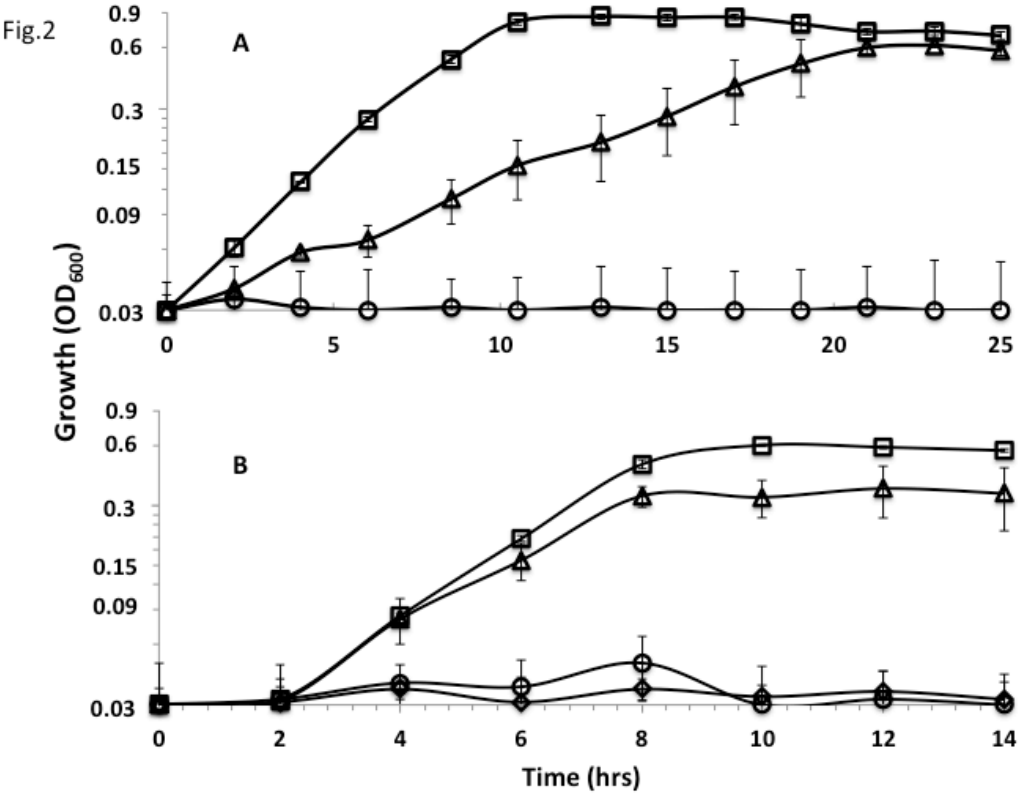

Figure 2. Growth curves with (A) lactate-sulfate and (B) lactate sulfite for *D. alaskensis* parent strain no addition (□) and with 5µM (△) or 20 µM (◇) TCS. Growth curve of the *rnf*A mutant with 5µM TCS (○) is also shown. Error bars show standard deviation.

Table 1(on next page)

Table 1.

Table 1. List of primers used for gap analysis in the *rnf* operon.

1 Table 1. List of primers used for gap analysis in the *rnf* operon.
2

Gap	**Forward primer**	**Reverse primer**
Gap CC (*cytC/rnfC*)	GGCATTCACGGCCTGTGCCT	CTTGTCGCCGGGGTGATCGG
Gap CD (*rnfC/rnfD*)	CCTGCTGGGACGCTACAGCG	ATGCCGTGTATGGTGCGCCC
Gap DG (*rnfD/rnfG*)	GGCAAGGCCGCCATGGTCAT	TGTACTCGGCCCCCGTGGAG
Gap GE (*rnfG/rnfE*)	ATCGGCTGCATGGTTGCCGT	ATTGGCGGACTTGGTGACCG
Gap EA (*rnfE/rnfA*)	GGGCTTGTTCTGGGCGCCAT	CCGCCCATGCCCAGACTGAC
Gap BE (*rnfB/rnfF*)	AAAGCCTGCCTCGCGTTCGG	AAGCCCCAGCAGACCGCATG

3

Table 2(on next page)

Table 2.

Table 2. Primers used for the RT-qPCR experiments.

1 Table 2. Primers used for the RT-qPCR experiments

Primer	Sequence	Target gene
Dde_587 forward	5'-AACCGTGGGTTATCGCCATT-3'	*rnfF* gene
Dde_587 reverse	5'-ATGGCTGTACATGCGTTTGC-3'	
Dde_589 forward	5'-AAGGGCAGGTAGTGCTGATG-3'	Putative regulator gene
Dde_589 reverse	5'-GGTAAACTTCACGCCTTCGC-3'	
Dde_590 forward	5'-GCCTGCGGCTTAATTTCGAG-3'	Cardiolipin synthase gene
Dde_590 reverse	5'-ACGGTTTTCCAGTTCGCTCA-3'	
16s forward	5'-ACGGTTGGAAACGACTGCTA-3'	16s rRNA gene
16s reverse	5'-AGCTAATCAGACGCGGACTC-3'	

2
3

Table 3(on next page)

Table 3.

Table 3. Normalized expression levels of genes within the *rnf* operon (from (Krumholz et al., 2015)). Expression was determined with the parent strain of *D. alaskensis* G20 during growth in pure culture with the indicated electron donors and acceptors and in coculture with *S. aciditrophicus* (SB) or with *S. wolfei* (SW) in the presence of benzoate or butyrate, respectively, as electron donors and sulfate as the electron acceptor.

Table 3. Normalized expression levels of genes within the *rnf* operon (from (Krumholz et al. 2015a)). Expression was determined with the parent strain of *D. alaskensis* G20 during growth in pure culture with the indicated electron donors and acceptors and in coculture with *S. aciditrophicus* (SB) or with *S. wolfei* (SW) in the presence of benzoate or butyrate, respectively, as electron donors and sulfate as the electron acceptor.

Gene	Function	Lactate/ Sulfate	H_2/ Sulfate	H_2/ Sulfite	SB	SW
Dde_0580	cyt c family protein	3.17	8.33	6.18	6.02	14.36
Dde_0581	RnfC subunit	3.05	6.68	6.12	5.61	13.50
Dde_0582	RnfD subunit	1.90	4.41	3.34	2.68	7.73
Dde_0583	RnfG subunit	2.83	6.35	5.19	5.43	10.07
Dde_0584	RnfE subunit	1.86	4.95	3.80	3.39	7.63
Dde_0585	RnfA subunit	2.24	5.78	4.23	2.98	8.41
Dde_0586	RnfB subunit	2.18	4.39	4.16	1.48	8.09
Dde_0587	RnfF subunit	2.20	4.90	5.25	1.94	10.15

Table 4(on next page)

Table 4.

Table 4. Gene expression in *D. alaskensis rnfA* and *rnf D* mutants relative to the parental strain using RT-qPCR. And normalized with the 16s rRNA gene.

Table 4. Gene expression in *D. alaskensis rnfA* and *rnf D* mutants relative to the parental strain using RT-qPCR. And normalized with the 16s rRNA gene.

Mutant type	Dde_587	Dde_589	Dde_590
rnf A	0.227±0.255	0.608±0.097	0.589±0.253
rnf D	1.955±0.624	1.155±0.078	0.972±0.420

Table 5(on next page)

Table 5. Magnitude of the ΔpH, ΔΨ and total proton motive force of the D. alaskensis G20 parent strain and the *rnfA* mutant growing on lactate and sulfate.

Table 5. Magnitude of the ΔpH, ΔΨ and total proton motive force of the D. alaskensis G20 parent strain and the *rnfA* mutant growing on lactate and sulfate. Standard deviation in parentheses. Value for the *rnfA* mutant were statistically different from the parent strain at $p<0.05$.

Table 5. Magnitude of the ΔpH, ΔΨ and total proton motive force of the D. alaskensis G20 parent strain and the *rnfA* mutant growing on lactate and sulfate. Standard deviation in parentheses. Value for the *rnfA* mutant were statistically different from the parent strain at $p<0.05$.

Measurement	Parent Strain	*rnf*A mutant
ΔΨ	-158 mV (2.1)	-117 mV (3.2)
ΔpH	0.43 (0.057)	0.29 (0.015)
PMF	-185 mV (3.1)	-135 mV (4.1)

Figure 1(on next page)

Figure 1-Growth curves of parent strain and mutants.

Figure 1. Growth curves on (A) lactate-sulfate (B) lactate-sulfite (C) pyruvate-sulfate and (D) formate-sulfate. Curves are for *D. alaskensis* parent strain (£) *rnf*A ( ) and *rnf*D (r) mutants. Error bars show standard deviation.

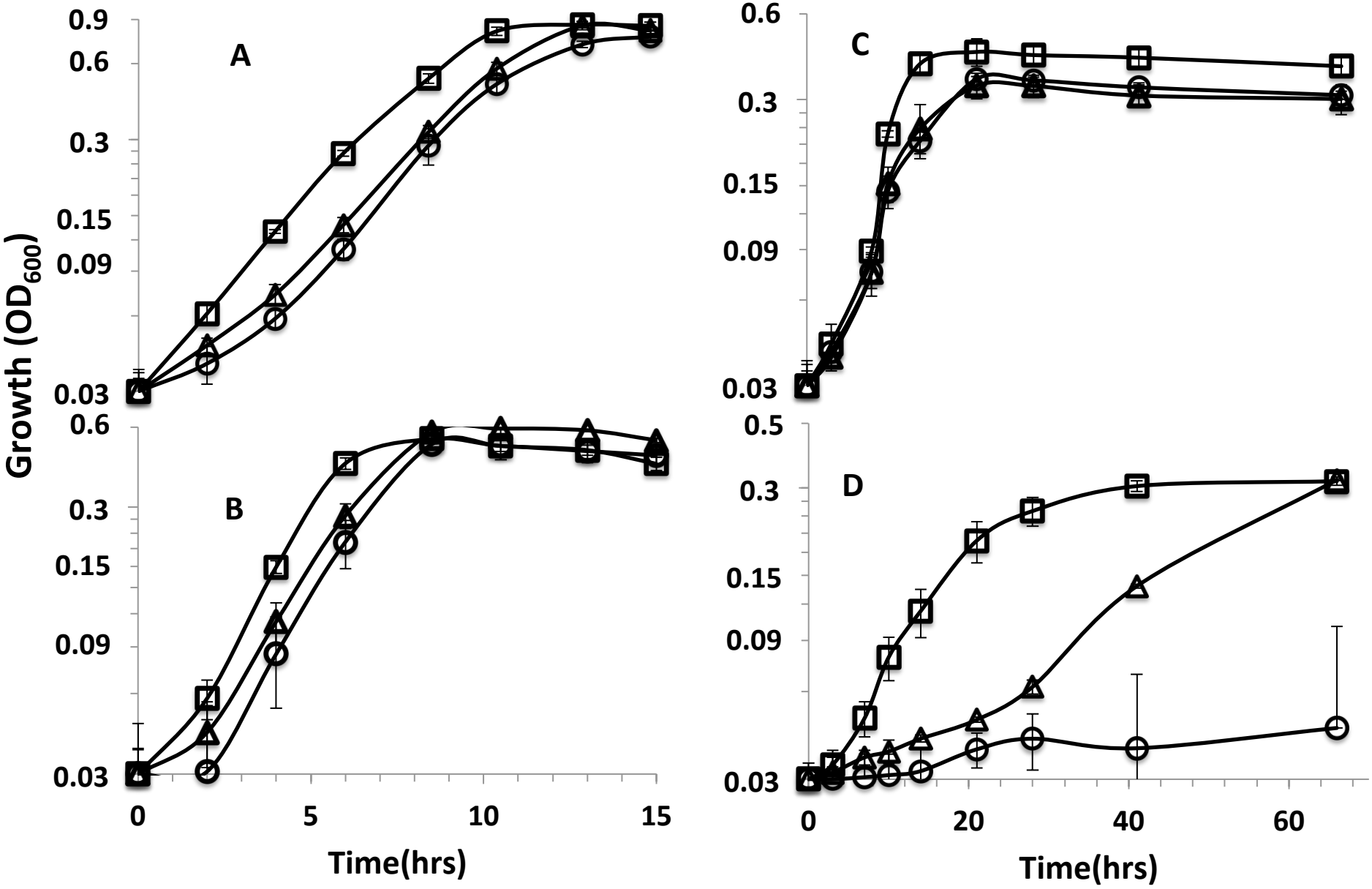
A
B
C
D
Growth (OD600)
Time(hrs)
Time(hrs)
0.9
0.6
0.3
0.15
0.09
0.03
0.6
0.3
0.15
0.09
0.03
0.6
0.3
0.15
0.09
0.03
0.5
0.3
0.15
0.09
0.03
0
5
10
15
0
20
40
60

Figure 2(on next page)

Figure 2. Effect of TCS on parent strain and mutants.

Figure 2. Growth curves with (A) lactate-sulfate and (B) lactate sulfite for *D. alaskensis* parent strain no addition (£) and with 5µM (r) or 20 µM (¯) TCS. Growth curve of the *rnf*A mutant with 5µM TCS ( ) is also shown. Error bars show standard deviation.

Fig.2

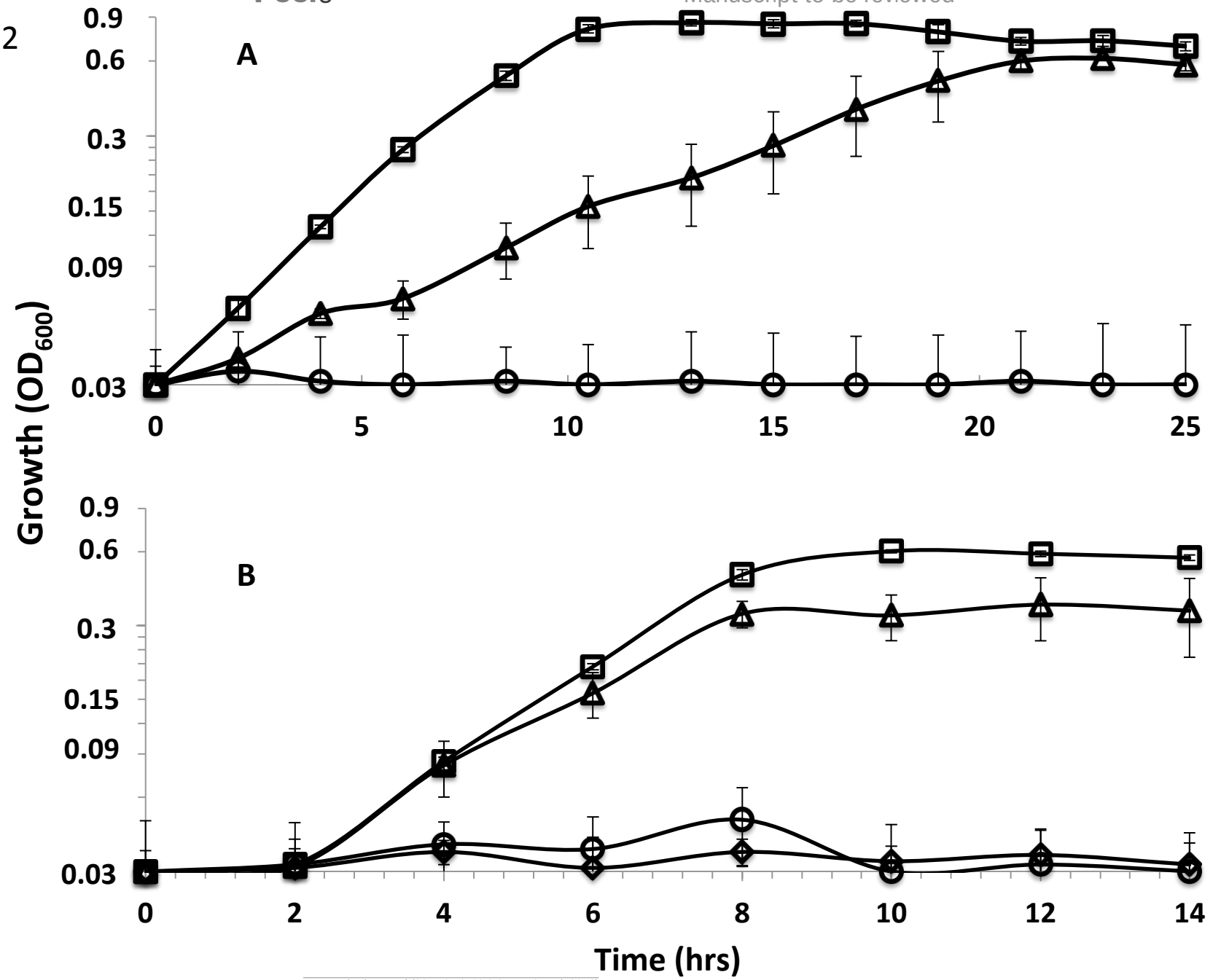
A
B
Growth (OD_{600})
0.9
0.6
0.3
0.15
0.09
0.03
0
5
10
15
20
25
2
4
6
8
12
14
Time (hrs)